with the result that the C-Mo-OH_2 angles are significantly smaller than 90°. On the other hand, this distortion in the $[WO(H_2O)(CN)_4]^{2-}$ ion together with the large trans effect of the oxo ligand, will promote dissociation of the aquo ligand and thus a dissociative reaction mode. This is in agreement with the positive value of $\Delta V^*(k_1)$. The large trans influence of the oxo ligand is clearly observed in the Mo-N bond distances in $[MoO(Phen)(CN)_3]^{-}$[6] (the corresponding tungsten complex is isomorphous with the molybdenum complex): The Mo-N bond distance trans to the oxo ligand is 2.363 (7) Å, whereas the Mo-N bond distance trans to the cyanide ligand is only 2.174 (7) Å.

Finally, the results of this investigation clearly demonstrate the close correlation between ground-state structure and transition-state energetics as facilitated by the trans effect of the oxo ligand.

Acknowledgment. The authors gratefully acknowledge financial support from the Deutsche Forschungsgemeinschaft, Fonds der Chemischen Industrie, the S.A. Council for Scientific and Industrial Research, and the Research Fund of the University of the Orange Free State.

Registry No. *trans*-$[WO_2(CN)_4]^{4-}$, 42720-52-5; *trans*-$[WO(H_2O)(CN)_4]^{2-}$, 105121-19-5; N_3^-, 14343-69-2.

Contribution from the Solar Energy Research Institute, Golden, Colorado 80401

Synthesis, Characterization, and Electrochemical Studies of Iron, Cobalt, and Nickel Complexes of Polyphosphine Ligands

Daniel L. DuBois* and Alex Miedaner

Received October 11, 1985

The reaction of $[M(CH_3CN)_6](BF_4)_2$ (where M = Fe, Co, and Ni) with $P(CH_2CH_2PPh_2)_3$ (PP_3), $PhP(CH_2CH_2PPh_2)_2$ (PP_2), and $Ph_2PCH_2CH_2PPh_2$ (dppe) results in the formation of $[Fe(PP_3)(CH_3CN)_2](BF_4)_2$, $[Fe(PP_2)(CH_3CN)_3](BF_4)_2$, $[Fe(dppe)_2(CH_3CN)_2](BF_4)_2$, $[Co(PP_3)(CH_3CN)](BF_4)_2$, $[Co(dppe)_2(CH_3CN)](BF_4)_2$, $[Ni(PP_3)(CH_3CN)](BF_4)_2$, $[Ni(PP_2)(CH_3CN)](BF_4)_2$, and $[Ni(dppe)_2](BF_4)_2$, respectively. Electrochemical studies have been carried out on these complexes to examine the influence of the nature of the polyphosphine ligand on the redox properties of each metal. For $[Fe(PP_3)(CH_3CN)_2](BF_4)_2$ the reversibility of both the Fe(II/III) and Fe(I/0) couples are enhanced relative to those of $[Fe(dppe)_2(CH_3CN)_2](BF_4)_2$. For $[Co(PP_3)(CH_3CN)](BF_4)_2$ the lowest oxidation state accessible in CH_3CN is +1, while for $[Co(dppe)_2(CH_3CN)](BF_4)_2$ the -1 oxidation state can be observed. The Ni(I/0) couple is reversible for $[Ni(dppe)_2](BF_4)_2$ and irreversible for $[Ni(PP_2)(CH_3CN)](BF_4)_2$ and $[Ni(PP_3)(CH_3CN)](BF_4)_2$. The electrochemical studies of the latter complex have led to the synthesis of a Ni(0) dimer, $[Ni(PP_3)]_2$.

Introduction

This paper is the first of a series investigating the electrochemical properties of transition-metal complexes containing polyphosphine ligands and their use as redox catalysts. Previous electrochemical investigations of metal complexes containing monodentate phosphine ligands have revealed that, in general, the reductions or oxidations of such complexes are irreversible due to cleavage or formation of metal-phosphorus bonds.[1] The use of chelating diphosphine ligands increases the reversibility of the redox couples of a number of metal complexes when compared to that of their monodentate analogues.[2-5] This tendency of a diphosphine ligand to promote reversible electron-transfer processes can be attributed to their ability to prevent metal-phosphorus bond cleavage. This suggests that other polyphosphine metal complexes may also display enhanced electrochemical reversibility by preventing metal-phosphorus bond cleavage.

By systematically varying the nature of the polyphosphine ligand in various metal complexes, we hope to gain a better understanding of the factors controlling the stability of different oxidation states of (polyphosphine)metal complexes. Such understanding could be useful in the rational development of metal phosphine complexes as redox catalysts. Currently transition-metal complexes of phosphine ligands are known to catalyze the electrochemical reduction of CO_2 to formic acid[6] and CO[7] and that of aryl halides to biaryls.[8]

In this paper we report the synthesis, characterization, and electrochemical studies of Fe, Co, and Ni complexes containing tetradentate, tridentate, and bidentate phosphine ligands as well as weakly coordinating acetonitrile ligands. These complexes permit a comparison of the ability of the various polyphosphine ligands to stabilize different oxidation states for a given metal.

Experimental Section

Acetonitrile and dichloromethane were dried by distillation from calcium hydride under nitrogen. Toluene and tetrahydrofuran (THF) were distilled from sodium benzophenone ketyl under nitrogen. Except where mentioned all reactions were carried out by using standard Schlenk techniques. All reagents and products were handled with exclusion of air with the exception of the air-stable nickel complexes. $P(CH_2CH_2PPh_2)_3$ (PP_3), $PhP(CH_2CH_2PPh_2)_2$ (PP_2), $Ph_2PCH_2CH_2PPh_2$ (dppe), and $Ni(COD)_2$ (COD is 1,5-cylooctadiene) were purchased from Strem Chemicals. The acetonitrile complexes of Fe, Co, and Ni were prepared as described in ref 9.

Infrared spectra were obtained on a Perkin-Elmer 599B spectrophotometer. All of the BF_4 salts showed a broad strong infrared absorption between 900-1150 cm^{-1}. A Varian E109 spectrometer was used for obtaining EPR spectra. All EPR spectra were recorded on 1×10^{-3} M dichloromethane solutions unless indicated otherwise. A JEOL FX90Q FT NMR spectrometer equipped with a tunable, variable-temperature probe was used to collect ^1H and ^{31}P NMR spectra. Me_4Si was used as an internal reference for all ^1H spectra. A capillary filled with phosphoric

(1) Bontempelli, G.; Magno, F.; Schiavon, G.; Corain, B. *Inorg. Chem.* **1981**, *20*, 2579. Bontempelli, G.; Magno, F.; Corain, B.; Schiavon, G. *J. Electroanal. Chem. Interfacial Electrochem.* **1979**, *103*, 243. Olson, D. C.; Keim, W. *Inorg. Chem.* **1969**, *8*, 2028. Pilloni, G.; Valcher, S.; *J. Electroanal. Chem. Interfacial Electrochem.* **1972**, *40*, 63. Pilloni, G.; Zotti, G.; Martelli, M. *J. Electroanal. Chem. Interfacial Electrochem.* **1975**, *63*, 424. Zotti, G.; Zecchin, S.; Pilloni, G. *J. Organomet. Chem.* **1983**, *246*, 61. Corain, B.; Bontempelli, G.; DeNardo, L.; Mazzocchin, G.-A. *Inorg. Chim. Acta* **1978**, *26*, 37. Jasinski, R. *J. Electrochem. Soc.* **1983**, *130*, 834.

(2) Sullivan, B. P.; Salmon, D. J.; Meyer, T. J. *Inorg. Chem.* **1978**, *17*, 3334. Pilloni, G.; Vecchi, E.; Martelli, M. *J. Electroanal. Chem. Interfacial Electrochem.* **1973**, *45*, 483. Pilloni, G.; Zotti, G.; Martelli, M. *Inorg. Chem.* **1982**, *21*, 1284. Kunin, A. J.; Nanni, E. J.; Eisenberg, R. *Inorg. Chem.* **1985**, *24*, 1852.

(3) Pilloni, G.; Zotti, G.; Martelli, M. *J. Electroanal. Chem. Interfacial Electrochem.* **1974**, *50*, 295.

(4) Zotti, G.; Zecchini, S.; Pilloni, G. *J. Organomet. Chem.* **1979**, *181*, 375.

(5) Martelli, M.; Pilloni, G.; Zotti, G.; Daolio, S. *Inorg. Chim. Acta* **1974**, *11*, 155. Bowmaker, G. A.; Boyd, P. D. W.; Campbell, G. K.; Hope, J. M. *Inorg. Chem.* **1982**, *21*, 1152. Zotti, G.; Pilloni, G.; Rigo, P.; Martelli, M. *J. Electroanal. Chem. Interfacial Electrochem.* **1981**, *124*, 277.

(6) Slater, S.; Wagenknecht, J. H. *J. Am. Chem. Soc.* **1984**, *106*, 5367.

(7) DuBois, D. L.; Miedaner, A. *J. Am. Chem. Soc.*, in press.

(8) Troupel, M.; Rollin, Y.; Sibille, S.; Fauvarque, J. F.; Perichon, J. *J. Chem. Res.* **1980**, 26. Schiavon, G.; Bontempelli, G.; Corain, B. *J. Chem. Soc., Dalton Trans.* **1981**, 1074.

(9) Hathaway, B. J.; Holah, D. G.; Underhill, A. E. *J. Chem. Soc.* **1962**, 2444.

0020-1669/86/1325-4642$01.50/0

acid was used as an external reference for ^{31}P NMR spectra. All ^{31}P NMR spectra were proton-decoupled. Electrochemical measurements were carried out with a Princeton Applied Research Model 173 potentiostat equipped with a Model 179 digital coulometer and a Model 175 universal programmer. A Houston Instruments Model 2000 X-Y recorder was used for plotting cyclic voltammograms. A silver wire was dipped in concentrated nitric acid, washed with distilled water, dipped in concentrated hydrochloric acid, and rinsed with distilled water. After drying, this wire was used as a pseudoreference electrode. This reference electrode was separated from the working and counter electrode compartments by a Vycor frit. Ferrocene was used as an internal standard. The potential of ferrocene vs. aqueous SCE in 0.2 N $LiClO_4$ solution of acetonitrile is reported to be +0.307 V.[10] All of our measurements were carried out in 0.3 N NEt_4BF_4 solutions of acetonitrile. In this solution we found the potential of ferrocene to be +0.40 V vs. aqueous SCE. A glassy-carbon disk electrode (IBM) was used as the working electrode, and a platinum wire was used as a counter electrode. All compounds were studied by cyclic voltammetry over a range of scan rates from 50 to 500 mV/s. Plots of i_p vs. $v^{1/2}$ were used to establish if the electron-transfer processes were under diffusion control. Elemental analyses were performed by Spang Microanalytical Laboratories.

$[FeP(CH_2CH_2PPh_2)_3(CH_3CN)_2](BF_4)_2$, $[Fe(PP_3)(CH_3CN)_2](BF_4)_2$. A colorless solution of $[Fe(CH_3CN)_6](BF_4)_2$ (0.95 g, 2.0 mmol) in acetonitrile (30 mL) was added to a solution of tris(2-(diphenylphosphino)ethyl)phosphine (1.34 g, 2.0 mmol) in dichloromethane (20 mL). The resultant red solution was stirred at room temperature for 30 min. The solvent was removed on a vaccum line to produce a red solid, which was recrystallized from acetone. The yield was 1.67 g (85%). ^1H NMR (acetone-d_6): Ph, 6.90–7.8 ppm (m); CH_3CN resonances, 3.41 (s) and 1.02 ppm (m); CH_2, 3.7–2.5 ppm (m). ^{31}P NMR (acetone-d_6) (see structure of **1** and text for discussion of assignments): P_c, 154.5 ppm (q, $J_{ac} = J_{bc} = 27$ Hz); P_b, 65.8 ppm (td, $J_{ab} = 37$ Hz); P_a, 49.91 ppm (dd). IR: no bands observed between 2100 and 2400 cm^{-1} for coordinated acetonitrile. Anal. Calcd for $C_{46}H_{48}N_2B_2F_8FeP_4$: C, 56.24; H, 4.94; N, 2.85; P, 12.61. Found: C, 56.09; H, 4.97; N, 2.86; P, 12.57.

$[FeP(CH_2CH_2PPh_2)_3(CH_3CN)]$, $[Fe(PP_3)(CH_3CN)]$. A solution of tetrahydrofuran (30 mL) and acetonitrile (30 mL) was added to a Schlenk flask containing $[Fe(CH_3CN)]_6](BF_4)_2$ (0.86 g, 1.81 mmol) and PP_3 (1.21 g, 1.81 mmol). The reaction mixture was stirred for 1 h, and then sodium amalgam containing 0.5 g of sodium was added. The reaction mixture was stirred for 2 h. During this time the solution turned a deep red-purple. The solution was filtered with a cannula, and the volume of the filtrate was reduced to approximately 30 mL in vacuo. The resulting black solid was collected by filtration and dried in a vaccum for 3 h. The yield was 0.67 g (48%). Due to the low solubility and instability of this complex in solution, it has not been possible to obtain reliable ^{31}P or ^1H NMR data for this complex. IR: CN stretch, 2202 cm^{-1}. Anal. Calcd for $C_{44}H_{45}NFeP_4$: C, 68.85; H, 5.91; N, 1.82. Found: C, 67.21; H, 5.88; N, 1.76.

$[FePhP(CH_2CH_2PPh_2)_2(CH_3CN)_3](BF_4)_2$, $[Fe(PP_2)(CH_3CN)_3](BF_4)_2$. A solution of $PhP(CH_2CH_2PPh_2)_2$ (1.07 g, 2.0 mmol) in dichloromethane (20 mL) was added to a solution of $[Fe(CH_3CN)_6](BF_4)_2$ (0.95 g, 2.0 mmol) in acetonitrile (30 mL). The resultant red solution was stirred for 2 h at room temperature, and the solvent was removed on a vaccum line to give a light red solid. The product was recrystallized from a dichloromethane/THF mixture by slowly removing the solvent. The product was collected by filtration and dried in vacuo. The yield was 1.42 g (80%). The product is a mixture of facial and meridional isomers. ^1H NMR (acetone-d_6): Ph, 7.0–8.1 ppm (m); CH_2, 2.5–3.5 ppm (m); CH_3CN resonances, 3.04, 2.76, 1.82, 1.53, and 1.61 ppm. ^{31}P NMR (acetone-d_6): central phosphorus atoms of facial and meridional isomers, 119.5 (t, $J = 30$ Hz) and 110.2 ppm (t, $J = 31$ Hz); terminal phosphorus atoms of facial and meridional isomers 66.9 (d) and 62.1 ppm (d). IR: CN stretches, 2250 (w), 2280 (w), and 2310 (w) cm^{-1}. Anal. Calcd for $C_{40}H_{42}N_3B_2F_8FeP_3$: C, 54.14; H, 4.78; N, 4.74; P, 10.51. Found: C, 53.83; H, 4.90; N, 4.57; P, 9.98.

$[Fe(Ph_2PCH_2CH_2PPh_2)_2(CH_3CN)_2](BF_4)_2$, $[Fe(dppe)_2(CH_3CN)_2](BF_4)_2$. A solution of $Ph_2PCH_2CH_2PPh_2$ (1.59 g, 4.0 mmol) in toluene (30 mL) was added to a solution of $[Fe(CH_3CN)_6](BF_4)_2$ (0.95 g, 2.0 mmol) in acetonitrile (20 mL). The red reaction mixture was stirred overnight, and the solvent was removed in vacuo to give a red powder. Two ^{31}P NMR resonances were observed at 50.6 (major product) and 74.2 ppm (minor product). The product was washed with dichloromethane (100 mL), and the filtrate was discarded. The remaining red product was recrystallized from acetone, and dried in vacuo at 50 °C for 5 h. The yield was 1.1 g (49%). ^1H NMR (dichloromethane-d_2): Ph, 6.9–7.5 ppm (m); CH_2, 3.01 ppm (m); CH_3CN, 1.91 ppm (m). ^{31}P NMR (acetonitrile-d_3): 50.6 ppm (s). IR: CN stretch, 2250 cm^{-1} (w). Anal. Calcd for $C_{56}H_{54}N_2B_2F_8FeP_4$: C, 60.67; H, 4.92; P, 11.18; N, 2.53. Found: C, 60.44; H, 4.72; P, 10.94; N, 2.39.

$[CoP(CH_2CH_2PPh_2)_3(CH_3CN)](BF_4)_2 \cdot CH_2Cl_2$, $[Co(PP_3)(CH_3CN)](BF_4)_2$. A red solution of $[Co(CH_3CN)_6](BF_4)_2$ (0.96 g, 2.0 mmol) in acetonitrile (30 mL) was added to a solution of PP_3 (1.34 g, 2.0 mmol) in dichloromethane (30 mL). The resultant dark green solution was stirred at room temperature for 30 min, and the solvent was removed in vacuo to produce a dark green solid. This solid was dissolved in dichloromethane (50 mL), and hexane (10 mL) was added. Cooling the flask to −20 °C overnight resulted in the precipitation of a dark green crystalline solid, which was collected by filtration and dried in vacuo at 50 °C for 8 h. The yield was 0.77 g (39%). An EPR spectrum recorded at room temperature in dichloromethane consisted of a broad doublet with $g = 2.11$ and $A = 90$ G. IR: CN stretches, 2275 (m) and 2315 (w) cm^{-1}. Anal. Calcd for $C_{45}H_{47}NB_2Cl_2CoF_8P_4$: C, 52.51; H, 4.60; N, 1.36; Co, 5.73; P, 12.04. Found: C, 52.78; H, 4.71; N, 1.37; Co, 5.91; P, 12.50.

$[CoP(CH_2CH_2PPh_2)_3(CH_3CN)](BF_4)$, $[Co(PP_3)(CH_3CN)](BF_4)$. Acetonitrile (30 mL) was added to a mixture of $[Co(CH_3CN)_6](BF_4)_2$ (0.90 g, 1.88 mmol) and PP_3 (1.26 g, 1.88 mmol). After the green reaction mixture was stirred for 0.5 h, zinc dust (0.4 g, 6.1 mmol) was added. The solution turned red within 5 min, and the mixture was stirred overnight. The reaction mixture was filtered to remove the zinc dust, and the solvent was removed from the filtrate *in vacuo* to yield a red-purple residue. This solid was dissolved in dichloromethane (30 mL) and filtered. Ethanol (30 mL) was added to the filtrate and the volume reduced to 20 mL by applying a vacuum. The resulting fine microcrystalline precipitate was collected by filtration and dried in vacuo for 3 h. The yield was 1.31 g (80%). ^1H NMR (acetonitrile-d_3): Ph, 7.16 ppm (s, br); CH_2, 3.5–1.5 ppm (m); CH_3CN, 1.95 ppm (s). ^{31}P NMR (acetonitrile-d_3): equatorial phosphorus atoms, 58.5 ppm (d, $J = 33$ Hz); apical phosphorus atom, 157.2 ppm (q). IR: CN stretch, 2245 cm^{-1} (w). Anal. Calcd for $C_{44}H_{45}NBCoF_4P_4$: C, 61.63; H, 5.29; N, 1.63. Found: C, 61.72; H, 5.42; N, 1.56.

$[Co(Ph_2PCH_2CH_2PPh_2)_2(CH_3CN)](BF_4)_2 \cdot CH_3OH$, $[Co(dppe)_2(CH_3CN)](BF_4)_2$. A solution of $[Co(CH_3CN)_6](BF_4)_2$ (1.08 g, 2.25 mmol) in acetonitrile (50 mL) was added to a solution of dppe (1.79 g, 4.5 mmol) in dichloromethane (70 mL). The reaction mixture was stirred for 1 h and the solvent removed in vacuo to produce an orange powder. Recrystallization from a mixture of dichloromethane and methanol yielded 1.26 g (50%) of an orange microcrystalline product. An EPR spectrum recorded at room temperature in dichloromethane consisted of a broad resonance with $g = 2.20$ and no resolved hyperfine splitting. IR: CN stretches, 2270 and 2310 cm^{-1}. Anal. Calcd for $C_{55}H_{55}NB_2CoF_8OP_4$: C, 59.92; H, 5.32; N, 1.27; Co, 5.34; P, 11.24. Found: C, 59.98; H, 5.38; N, 1.48; Co, 5.51; P, 12.13.

$[NiP(CH_2CH_2PPh_2)_3(CH_3CN)](BF_4)_2$, $[Ni(PP_3)(CH_3CN)](BF_4)_2$. An acetonitrile solution (20 mL) of $[Ni(CH_3CN)_6](BF_4)_2 \cdot {}^1/_2CH_3CN$ (1.00 g, 2.0 mmol) was added to a dichloromethane solution (30 mL) of $P(CH_2CH_2PPh_2)_3$ (1.34 g, 2.0 mmol). The resulting purple solution was stirred at room temperature for 1 h, and the solvent was removed on a rotary evaporator. The crude product was dissolved in dichloromethane (100 mL) in air, and the solution was filtered. Ethanol (100 mL) was added to the filtrate, and the volume of the solution was reduced to ~50 mL on a rotary evaporator. The deep purple microcrystalline product that formed was collected by filtration and dried in vacuo. The yield was 1.70 g (94%). ^1H NMR (dichloromethane-d_2): Ph, 7.2–7.4 ppm (m); CH_2CH_2, 2.72 (m) and 2.91 ppm (m); CH_3CN, 2.34 ppm (q, $^5J_{PH} = 2$ Hz). ^{31}P NMR (acetonitrile-d_3): central phosphorus atom, 146.3 ppm (q, $^2J = 27$ Hz); terminal phosphorus atoms, 44.4 ppm (d). IR: CN stretches, 2310 (w) and 2285 (m) cm^{-1}. Anal. Calcd for $C_{44}H_{45}NB_2F_8NiP_4$: C, 55.98; H, 4.81; N, 1.48; F, 16.09; P, 13.12. Found: C, 55.94; H, 4.70; N, 1.44; F, 15.92; P, 12.72.

$[NiPhP(CH_2CH_2PPh_2)_2(CH_3CN)](BF_4)_2$, $[Ni(PP_2)(CH_3CN)](BF_4)_2$. A blue solution of $[Ni(CH_3CN)_6](BF_4)_2 \cdot {}^1/_2CH_3CN$ (1.00 g, 2.0 mmol) in CH_3CN (20 mL) was added to a dichloromethane solution (50 mL) of $PhP(CH_2CH_2PPh_2)_2$ (1.07 g, 2.0 mmol). The resultant red solution was stirred for 1 h, and the solvent was removed in vacuo. The crude product was redissolved in dichloromethane (50 mL), and ethanol (70 mL) was added. A yellow precipitate was obtained by reducing the volume of the solution to ~20 mL in vacuo. The yellow precipitate was collected by filtration and dried on a vacuum line at 50 °C for 5 h. The yield was 1.4 g (86%). ^1H NMR (dichloromethane-d_2): Ph, 7.4–7.8 ppm; CH_2CH_2, 2.4–3.5 ppm; CH_3CN, 2.05 ppm (br s). ^{31}P NMR (acetonitrile-d_3): terminal phosphorus atoms, 55.7 ppm (d, $J = 50$ Hz); central phosphorus atom, 108.8 ppm (t). IR: CN stretches, 2310 (w) and 2280 (m) cm^{-1}. Anal. Calcd for $C_{36}H_{36}NB_2F_8NiP_3$: C, 53.52; H, 4.50; N, 1.73; F, 18.81; P, 11.50. Found: C, 53.54; H, 4.51; N, 1.67; F, 18.79; P, 11.63.

(10) Bard, A. J.; Faulkner, L. R. *Electrochemical Methods*; Wiley: New York, 1980; pp 701, 35, 433, and 451–453.

$[NiP(CH_2CH_2PPh_2)_3]_2$, $[Ni(PP_3)]_2$. A cold (−80 °C) THF solution (50 mL) of $Ni(COD)_2$ (0.83 g, 3.0 mmol) was added via cannula to a cold (−80 °C) THF solution (50 mL) of $P(CH_2CH_2PPh_2)_3$ (2.0 g, 3.0 mmol). Warming the reaction mixture slowly to room temperature resulted in a clear orange solution. The solvent was removed in vacuo to produce a yellow solid, which was washed with hexanes. The solid was collected by filtration and dried in vacuo at 50 °C for 2 h. The yield was 1.95 g (89%). ^1H NMR (toluene-d_8): Ph, 6.9–7.9 ppm (m); CH_2CH_2, 1.2–2.8 ppm (m). ^{31}P NMR: (see structure **4** of text for labeling of P atoms) P_a, 33.6 ppm (ddt, J_{ac} = 49 Hz, $J_{ac'}$ = 49 Hz; J_{ab} = 20 Hz); P_b, 42.4 ppm (dd, J_{bc} = 46 Hz); P_c, 59.6 ppm (ddt). Anal. Calcd for $C_{42}H_{42}NiP_4$: C, 69.15; H, 5.82; P, 16.98. Found: C, 69.28; H, 5.83; P, 17.08.

$[NiP(CH_2CH_2PPh_2)_3](BF_4)$, $[Ni(PP_3)](BF_4)$. $[Ni(PP_3)(CH_3CN)](BF_4)_2$ (0.45 g, 0.50 mmol), $Ni(COD)_2$ (0.14 g, 0.50 mmol), and $P(CH_2CH_2PPh_2)_3$ (0.34 g, 0.50 mmol) were placed in a 250-mL Schlenk flask. THF (100 mL) was added, and the reaction mixture was stirred for 20 h. A light lavender product precipitated during this period. The solid was collected by filtration and dried in vacuo for 2 h at 50 °C. The yield was 0.76 g (93%). An EPR spectrum recorded at room temperature of the solid consisted of a broad resonance with g = 2.09. IR spectrum: BF_4 stretches, 950–1150 cm^{-1}. The product is not soluble in THF or hydrocarbons. It reacts rapidly with halogenated solvents and is pyrophoric in air. The product disproportionated in CH_3CN to form $[NiP(CH_2CH_2PPh_2)_3(CH_3CN)](BF_4)_2$ and $[NiP(CH_2CH_2PPh_2)_3]_2$. Both products were characterized by ^{31}P NMR spectroscopy.

Results

Synthesis and Characterization of Metal Complexes. The reaction of anhydrous metal acetonitrile complexes with polyphosphine ligands provides a general route to the synthesis of (polyphosphine)metal complexes containing weakly bound acetonitrile ligands. Reaction of PP_3 (where PP_3 is $P(CH_2CH_2PPh_2)_3$) with $[Fe(CH_3CN)_6](BF_4)_2$, eq 1, results in nearly quantitative

$$[Fe(CH_3CN)_6](BF_4)_2 + PP_3 \rightarrow [Fe(PP_3)(CH_3CN)_2](BF_4)_2 \quad (1)$$

formation of $[Fe(PP_3)(CH_3CN)_2](BF_4)_2$ as shown by ^{31}P NMR spectra of the crude reaction product. A mixture of facial and meridional isomers of $[Fe(PP_2)(CH_3CN)_3](BF_4)_2$ is formed from the reaction of $[Fe(CH_3CN)_6](BF_4)_2$ and PP_2 (where PP_2 is $PhP(CH_2CH_2PPh_2)_2$). Two products are formed when $[Fe(CH_3CN)_6](BF_4)_2$ is reacted with dppe (where dppe is $Ph_2PCH_2CH_2PPh_2$). Only one product, *trans*-$[Fe(dppe)_2(CH_3CN)_2](BF_4)_2$, has been characterized. The identity of the other product of this reaction has not been determined.

All three iron complexes are red or red-orange solids that are sensitive to air in the solid state and in solution. They are quite soluble in acetonitrile and acetone and slightly soluble in dichloromethane. All three compounds decompose in dimethyl sulfoxide due to displacement of the phosphine ligands as indicated by their ^{31}P NMR spectra.

The ^{31}P NMR spectrum of $[Fe(PP_3)(CH_3CN)_2](BF_4)_2$ (**1**) is consistent with a low-spin octahedral complex with the two acetonitrile ligands occupying cis positions. A quartet is observed

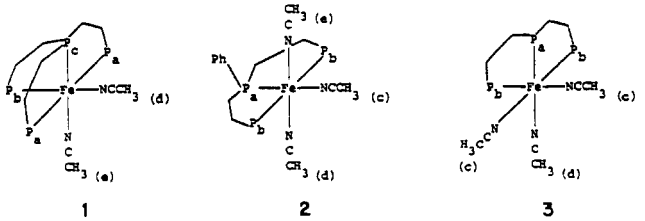

1 **2** **3**

for the central phosphorus atom of the ligand, P_c, due to equal coupling to the three cis phosphorus atoms. The resonance for the mutually trans phosphorus atoms of the ligand, P_a, appears as a doublet of doublets due to coupling to the central phosphorus atom and the remaining terminal phosphorus atom, P_b. The resonance for the latter phosphorus atom appears as a triplet of doublets. This pattern arises from the coupling to the two mutually trans phosphorus atoms, P_a, and the central phosphorus atom, P_c. The coupling of P_c to P_a and P_b is smaller than the coupling of P_a to P_b. This phenomenon is attributed to coupling through the two carbon backbone of the ligand, decreasing the coupling that occurs through the metal atom, as has been observed previously.[11]

No bands assignable to CN stretches are observed in the infrared spectrum of $[Fe(PP_3)(CH_3CN)_2](BF_4)_2$. However, ^1H NMR spectra taken in acetone-d_6 show two methyl resonances at 3.41 and 1.02 ppm, which are assigned to coordinated acetonitrile. If the spectrum is recorded with acetonitrile-d_3 as the solvent, the resonance at 1.02 ppm shifts to the position of free acetonitrile. This indicates that one of the acetonitrile ligands is labile and exchanges with solvent within the time of sample preparation. The remaining acetonitrile ligand exchanges with CD_3CN with a half-life of approximately 5 h at room temperature.

The reduction of $[Fe(PP_3)(CH_3CN)_2](BF_4)_2$ with sodium amalgam in a mixture of tetrahydrofuran and acetonitrile results in the formation of the Fe(0) complex $[Fe(PP_3)(CH_3CN)]$. Elemental analysis confirms the basic composition of this complex, and the infrared spectrum has an absorption at 2205 cm^{-1}, which is assigned to coordinated acetonitrile. The relatively low CN stretching frequency of the coordinated acetonitrile is a reflection of the low oxidation state of iron. Cyclic voltammetry and coulometry experiments discussed below confirm an Fe(0) oxidation state for this complex.

The ^{31}P NMR spectrum of the product obtained from the reaction of $[Fe(CH_3CN)_6](BF_4)_2$ with PP_2 consists of two doublets and two triplets of approximately equal intensity. The triplet resonances at 119.5 and 110.2 ppm are assigned to the central phosphorus atoms, P_a, of the meridional (**2**) and facial (**3**) isomers. Similarly, the doublets observed at 66.9 and 62.1 ppm are assigned to the terminal phosphorus atoms, P_b, of **2** and **3**. Because of the nearly equal intensities of the two doublets and two triplets no assignment can be made of specific resonances to either isomer.

^1H NMR spectra recorded on acetone-d_6 solutions of $[Fe(PP_2)(CH_3CN)_3](BF_4)_2$ show five methyl resonances assigned to coordinated acetonitrile at 3.04, 2.76, 1.82, 1.61, and 1.53 ppm. Four of the resonances are of nearly equal intensity, while the resonance at 1.82 ppm is twice as intense as the others. Three of the resonances arise from the three different acetonitrile ligands present in the meridional isomer (**2**). The acetonitrile ligands d and e of isomer **2** are not equivalent since the phenyl group attached to the central phosphorus atom is directed toward ligand e and away from d. This type of nonequivalence has been observed previously for Rh and Mo complexes containing $PhP(CH_2CH_2CH_2PPh_2)_2$ and PP_2, respectively.[12,13] The remaining two resonances can be assigned to the facial isomer (**3**) with the resonance for acetonitrile ligands c being twice as intense as the resonance for d. Due to its intensity, the resonance at 1.82 ppm can be assigned unambiguously to ligands c of the facial isomer (**3**). In acetonitrile-d_3 this latter resonance shifts to the position of uncoordinated acetonitrile within the time required to prepare the NMR sample, indicating that the corresponding acetonitrile ligands are labile. The remaining acetonitrile resonances are replaced by deuterioacetonitrile with half-lives ranging from approximately 0.5 to 3 h. In contrast to $[Fe(PP_3)(CH_3CN)_2](BF_4)_2$, *fac*- and *mer*-$[Fe(PP_2)(CH_3CN)_3](BF_4)_2$ have three weak infrared absorptions corresponding to CN stretches of coordinated acetonitrile at 2250, 2280, and 2310 cm^{-1}.

The complex *trans*-$[Fe(dppe)_2(CH_3CN)_2](BF_4)_2$ can be isolated from the crude product obtained from the reaction of $[Fe(CH_3CN)_6](BF_4)_2$ and dppe by washing with dichloromethane and crystallization of the residue from acetone. The perchlorate salt has been prepared previously by other workers from $[Fe(H_2O)_6](ClO_4)_2$ and dppe in acetonitrile.[3] On the basis of the observation of a single infrared stretch for coordinated acetonitrile at 2235 cm^{-1}, a trans geometry was assigned to this compound. The BF_4 salt similarly has only one weak infrared stretch at 2250 cm^{-1}, and the ^{31}P NMR spectrum has a single resonance at 55 ppm, consistent with a trans geometry. In acetone-d_6 the methyl resonance for coordinated acetonitrile is an unresolved multiplet

(11) Garrou, P. E. *Chem. Rev.* **1981**, *81*, 229.
(12) Meek, D. W.; DuBois, D. L.; Tiethof, J. *Adv. Chem. Ser.* **1976**, *No. 150*, 335.
(13) George, T. A.; Howell, D. B. *Inorg. Chem.* **1984**, *23*, 1502.

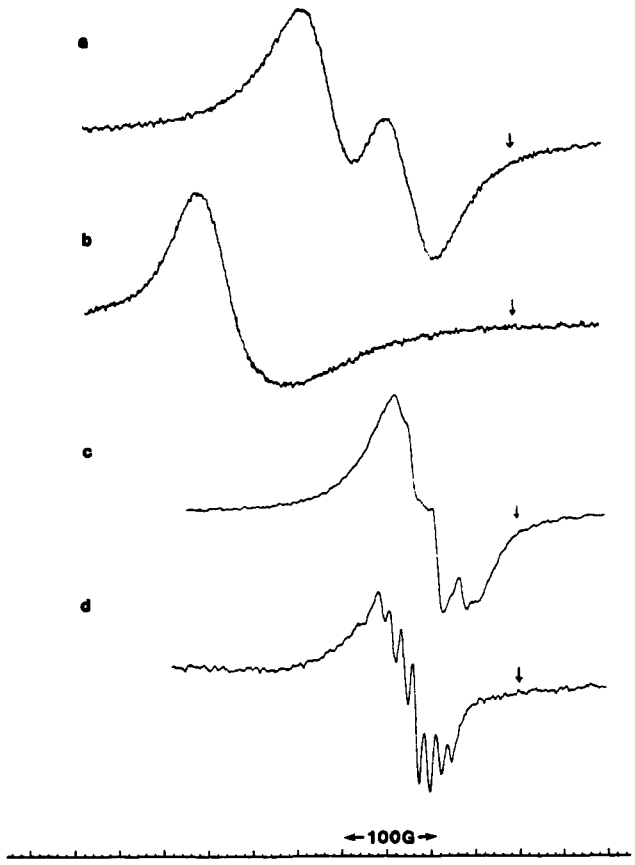

Figure 1. X-Band EPR spectra of 1.0×10^{-3} M solutions of (a) $[Co(PP_3)(CH_3CN)](BF_4)_2$ in CH_2Cl_2, (b) $[Co(dppe)_2(CH_3CN)](BF_4)_2$ in CH_2Cl_2, (c) $[Fe(PP_3)(CH_3CN)](BF_4)$ in THF, and (d) $[Fe(dppe)_2(CH_3CN)](BF_4)$ in THF. Arrow indicates $g = 2.00$.

at 1.95 ppm. The multiplet structure arises from the coupling of the methyl protons of acetonitrile to phosphorus. In acetonitrile-d_3 the resonance occurs at the position of free acetonitrile, but no multiplet structure is observed. These observations are consistent with labile acetonitrile ligands for this complex.

Reaction of $[Co(CH_3CN)_6](BF_4)_2$ with PP_3 and dppe results in the formation of a green five-coordinate complex, $[Co(PP_3)(CH_3CN)](BF_4)_2$, and a yellow five-coordinate complex, $[Co(dppe)_2(CH_3CN)](BF_4)_2$, respectively. Although a green solid can be isolated from the reaction of PP_2 with $[Co(CH_3CN)_6](BF_4)_2$, repeated efforts to obtain analytically pure samples from this reaction were unsuccessful. $[Co(PP_3)(CH_3CN)](BF_4)_2$ and $[Co(dppe)_2(CH_3CN)](BF_4)_2$ are moderately air sensitive in solution and the solid state. They are soluble in acetonitrile and dichloromethane and insoluble in nonpolar organic solvents and ethanol.

The formulation of $[Co(PP_3)(CH_3CN)](BF_4)_2$ as a low-spin, five-coordinate cobalt(II) complex is based on the following data. Elemental analysis indicates the presence of one acetonitrile ligand per cobalt atom. Two infrared bands are observed at 2275 and 2315 cm^{-1}, consistent with the presence of coordinated acetonitrile. Both bands are present in solution, and there is no evidence for isomers since the ultraviolet and visible spectra are the same in acetonitrile, dichloromethane, and acetone. There is also no evidence for dissociation of acetonitrile since Beer's law is obeyed over the concentration range of 1×10^{-2} to 1×10^{-4} M in dichloromethane. On the basis of these data the weak band at 2315 cm^{-1} is assigned to a combination band. Such bands are commonly observed in this region for acetonitrile complexes.[14] The room-temperature EPR spectrum of a 1×10^{-3} M solution of $[Co(PP_3)(CH_3CN)](BF_4)_2$ in dichloromethane is shown in Figure 1a. It consists of a broad doublet with a g value of 2.11 and a phosphorus hyperfine coupling constant of 90 G. The value of the hyperfine coupling constant is larger than the ~20 G value observed in other five-coordinate Co(II) phosphine complexes.[15,16] Hyperfine coupling for cobalt or for the three remaining phosphorus atoms is not resolved. The observation of a room-temperature EPR spectrum and the coupling of the electron to only one phosphorus nucleus are consistent with a five-coordinate complex of low symmetry. The closely related complexes, $[Co(PP_3)(H_2O)](BF_4)_2$ and $[Co(PP_3)(OH)](BF_4)$, have been characterized by X-ray structure determinations. These cations have square-pyramidal geometries.[17]

The reduction of $[Co(PP_3)(CH_3CN)](BF_4)_2$ with zinc results in the formation of the Co(I) complex $[Co(PP_3)(CH_3CN)](BF_4)$. The ^{31}P NMR spectrum in acetonitrile consists of a doublet at 58.5 ppm and a quartet at 157.2 ppm, which are assigned to equatorial and apical phosphorus atoms, respectively, of a trigonal bipyramid. The presence of coordinated acetonitrile is confirmed by the observation of a methyl resonance at 1.44 ppm in the ^1H NMR spectrum recorded in dichloromethane-d_2. In acetonitrile-d_3 the resonance occurs at the position of uncoordinated acetonitrile and indicates the acetonitrile ligand is labile in the time required to prepare the NMR sample and collect the spectrum. The CN stretching vibration is observed at 2245 cm^{-1} in the infrared spectrum. This is 30 cm^{-1} lower than for its Co(II) analogue and is consistent with either weaker σ bonding of the ligand to Co(I) or stronger π back-bonding.

The complex $[Co(dppe)_2(CH_3CN)](BF_4)_2$ analyzes correctly for one acetonitrile and two dppe ligands per cobalt atom, consistent with a coordination number of five. The solution EPR spectrum obtained at room temperature consists of a single, broad, asymmetric resonance (see Figure 1b) with a g value of 2.20. This g value is very similar to the g values of other five-coordinate Co(II) complexes.[16] No cobalt or phosphorus hyperfine coupling is observed in contrast to the room-temperature EPR spectra of $[Co(dppe)_2](BPh_4)$[15] and the five-coordinate $[Co(dppe)_2X]X$ complexes (where X is a halogen).[16] The failure to observe phosphorus hyperfine coupling for $[Co(dppe)_2(CH_3CN)](BF_4)_2$ may be due to broadening caused by additional hyperfine coupling to the nitrogen atom of the coordinated acetonitrile as observed for $[Fe(dppe)_2(CH_3CN)](BF_4)$ described below.

Two bands are observed at 2310 and 2270 cm^{-1} in the infrared spectrum of $[Co(dppe)_2(CH_3CN)](BF_4)_2$. The weak absorption at 2310 cm^{-1} is assigned to a combination band of the coordinated acetonitrile, while the more intense band at 2270 cm^{-1} is assigned to the CN stretching vibration. Both bands are present in solution; therefore, the presence of a second band cannot be attributed to solid-state effects. These two bands could also arise from two different isomers of $[Co(dppe)_2(CH_3CN)](BF_4)_2$. The observation of similar infrared spectra of $[Co(PP_3)(CH_3CN)](BF_4)_2$ and the nickel complexes described below, in which no isomers are present, lead us to prefer the interpretation in which the band at 2310 cm^{-1} is assigned to a combination band.

Reaction of $[Ni(CH_3CN)_6](BF_4)_2$ with PP_3, PP_2, and dppe yields $[Ni(PP_3)(CH_3CN)](BF_4)_2$, $[Ni(PP_2)(CH_3CN)](BF_4)_2$, and $[Ni(dppe)_2](BF_4)_2$,[18] respectively. The latter two complexes are assigned square-planar structures and are yellow, while the first is assigned a trigonal-bipyramidal structure and is deep purple. All three complexes are diamagnetic. They are air stable, soluble in acetonitrile, dichloromethane, and acetone, and insoluble in nonpolar organic solvents.

The ^{31}P NMR spectrum of $[Ni(PP_3)(CH_3CN)](BF_4)_2$ consists of a doublet for the terminal phosphorus atoms and a quartet for the central phosphorus atom of the tetradentate ligand. This splitting pattern is consistent with a trigonal-bipyramidal structure in which the central phosphorus atom occupies an axial position and the terminal phosphorus atoms all occupy equatorial positions.

(14) Storhoff, B. N.; Lewis, C. H., Jr. *Coord. Chem. Rev.* **1977**, *23*, 1.
(15) Attanasio, D. *Chem. Phys. Lett.* **1977**, *49*, 547.
(16) Sethulakshmi, C. N.; Manoharan, P. T. *Inorg. Chem.* **1981**, *20*, 2533.
(17) Orlandini, A.; Sacconi, L. *Inorg. Chem.* **1976**, *15*, 78.
(18) Hudson, M. J.; Nyholm, R. S.; Stiddard, M. H. B. *J. Chem. Soc. A* **1968**, 40. Sacco, A.; Gorieri, F. *Gazz. Chim. Ital.* **1963**, *93*, 687. Horrocks, W. D., Jr.; Van Hecke, G. R.; Hall, D. D. *Inorg. Chem.* **1967**, *6*, 694. Morassi, R.; Dei, A. *Inorg. Chim. Acta* **1972**, *6*, 314.

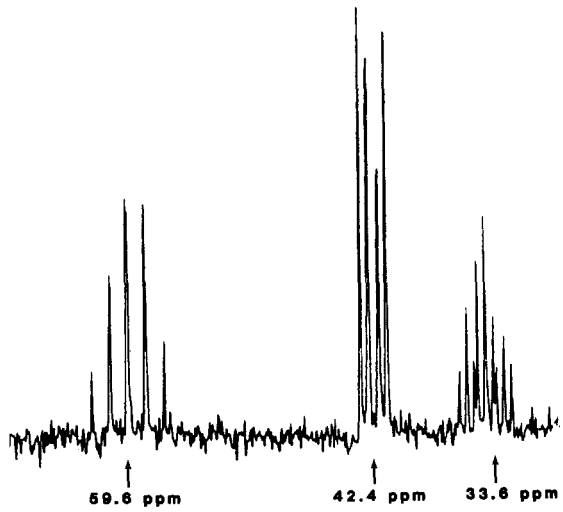

Figure 2. Proton-decoupled ^{31}P NMR spectrum of $[Ni(PP_3)]_2$ in THF.

The ^1H NMR spectrum in dichloromethane-d_2 exhibits a quartet resonance ($^5J_{PH}$ = 2 Hz) at 2.34 ppm, which is assigned to coordinated acetonitrile. It is interesting that the coupling of the methyl protons is stronger to the cis phosphorus atoms and no coupling is observed to the trans phosphorus atom. In acetonitrile-d_3 this resonance shifts to the position of free acetonitrile and the coupling is no longer observed, consistent with a labile acetonitrile ligand. The infrared spectrum shows a medium-intensity band at 2285 cm^{-1}, assigned to the CN stretching vibration of the coordinated acetonitrile ligand, and a weak band at 2310 cm^{-1}. The latter band is assigned to a combination band since it is observed for spectra recorded on solutions as well as on solid samples, and ^{31}P and ^1H NMR spectra indicate the presence of only one complex in solution.

The ^{31}P NMR spectrum of $[Ni(PP_2)(CH_3CN)](BF_4)_2$ consists of a doublet and a triplet as expected for a square-planar complex. The elemental analysis indicates the presence of one acetonitrile ligand per molecule. The acetonitrile ligand is labile as indicated by its appearance as a sharp singlet at 1.96 ppm in acetonitrile-d_3 compared with a broad singlet at 2.05 ppm in dichloromethane-d_2. The infrared spectrum also indicates the presence of coordinated acetonitrile by the presence of a weak band at 2310 cm^{-1} and a medium-intensity band at 2280 cm^{-1}. By use of the criteria discussed above, the weak band at 2310 cm^{-1} is again assigned to a combination band while the band at 2280 cm^{-1} is assigned to the CN stretching vibration.

The preparation, characterization, and electrochemical data of various salts of the $[Ni(dppe)_2]^{2+}$ cation have been described in detail by others.[5,18] However, our electrochemical data on $[Ni(dppe)_2](BF_4)_2$ are reported in Table I for purposes of comparison with $[Ni(PP_3)(CH_3CN)](BF_4)_2$ and $[Ni(PP_2)(CH_3CN)](BF_4)_2$.

In order to characterize the products of the electrochemical reduction of $[Ni(PP_3)(CH_3CN)](BF_4)_2$, the complexes $[Ni(PP_3)]_2$ and $[Ni(PP_3)]BF_4$ have been prepared by alternate methods. The reaction of $Ni(COD)_2$ with PP_3 in THF results in the clean formation of the Ni(0) dimer $[Ni(PP_3)]_2$. The same complex can be prepared by reduction of $[Ni(PP_3)(CH_3CN)](BF_4)_2$ with magnesium in THF or by bulk electrolysis. The ^{31}P NMR spectrum of $[Ni(PP_3)]_2$ shown in Figure 2 is consistent with dimeric structure **4**, which has three phosphorus atoms of the

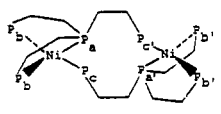

4

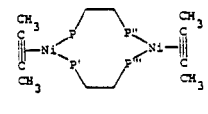

5

tetradentate ligand coordinated to one nickel atom with the fourth phosphorus atom bridging to the second nickel atom.

The resonance corresponding to P_a of **4** occurs at 33.6 ppm and is split into a doublet by P_c (J_{ac} = 49 Hz). This doublet is in turn split into a doublet by the coupling of P_a to $P_{c'}$ ($J_{ac'}$ = 49 Hz). The 49 Hz value of the coupling constant for $J_{ac'}$ is similar to the 45.6 Hz coupling between the P′ and P″ of **5**.[19] Since $J_{ac} = J_{ac'}$ a triplet pattern is observed. This triplet is further split into a triplet by the coupling of P_a to the two P_b nuclei (J_{ab} = 20 Hz). The resonance occurring at 42.4 ppm is assigned to P_b, which is split into a doublet of doublets by P_c (J_{bc} = 46 Hz) and P_a. The resonance centered at 59.6 ppm is assigned to P_c, which couples nearly equivalently to $P_{a'}$, P_b, and P_a to produce a quintet pattern, which can also be analyzed as a doublet of doublet of triplets. The observed splitting patterns are the same at both 32.6 and 101.3 MHz, indicating that all splitting is due to coupling. The assignment of the resonance at 33.6 ppm to the central phosphorus atom P_a rather than the bridging terminal phosphorus atom, $P_{c'}$ is based on the observation that the coupling of P_a to P_b is smaller than the coupling of P_a to P_c. This is expected since the coupling between phosphorus atoms connected by the two-carbon chain of the tetradentate ligand is normally smaller than the coupling observed for nuclei that are not connected by a two-carbon chain.[11] Although the ^{31}P NMR data are the most diagnostic, the elemental analysis and ^1H NMR data given in the Experimental Section are consistent with the formulation of this complex.

Scheme I

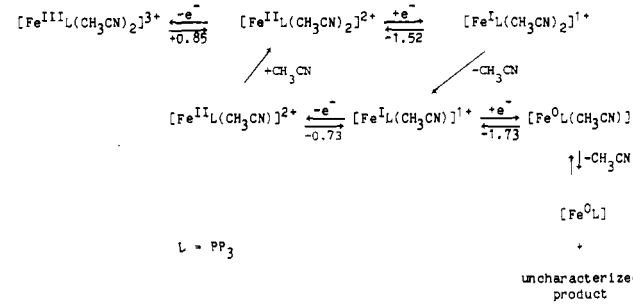

Precedent for dimeric Ni(0) structures may be found in the synthesis of **5** and related dimers.[19] The closely related complex $[Ni(NP_3)]$ (where NP_3 is $N(CH_2CH_2PPh_2)_3$) has been structurally characterized by a single-crystal X-ray diffraction study.[20] This complex is monomeric and has a trigonal-pyramidal structure with the nitrogen atom occupying the apical position. The structural differences between $[Ni(NP_3)]$ and $[Ni(PP_3)]_2$ are most likely due to the increased ring strain, which would be present in $[Ni(PP_3)]$ due to the longer Ni–P bond compared to a Ni–N bond. The increased strain results in ring opening of $[Ni(PP_3)]$ and subsequent dimer formation.

The reaction of $[Ni(PP_3)]_2$ with 2 equiv of $[Ni(PP_3)(CH_3CN)](BF_4)_2$ in THF yields the Ni(I) monomer $[Ni(PP_3)](BF_4)$. This complex has the same physical and chemical properties as those of $[Ni(PP_3)](ClO_4)$, which was isolated from the reaction of $[Ni(C_2H_4)(PPh_3)_2]$, PP_3, and $(C_3Ph_3)(ClO_4)$ and characterized by an X-ray structure determination.[21]

Electrochemical Studies of Fe Complexes. The electrochemical studies carried out on $[Fe(PP_3)(CH_3CN)_2](BF_4)_2$ and its reduction products are consistent with the reactions shown in Scheme I. The cyclic voltammogram of $[Fe(PP_3)(CH_3CN)_2](BF_4)_2$, Figure 3a, exhibits a quasi-reversible, diffusion-controlled, one-electron oxidation for the Fe(II/III) couple at +0.85 V vs. ferrocene with a peak to peak separation of 80 mV and an i_{pa}/i_{pc} ratio of 0.95. Controlled-potential electrolysis of an acetonitrile solution of $[Fe(PP_3)(CH_3CN)](BF_4)_2$ at +1.05 V vs. ferrocene using a reticulated pyrolytic graphite electrode results in the passage of more than three electrons per iron atom. The nature of the redox process

(19) Pörschke, K. R.; Mynott, R.; Angermund, R.; Krüger, C. *Z. Naturforsch., B: Anorg. Chem., Org. Chem.* **1985**, *40B*, 199. Pörschke, K. R.; Nynott, R.; Krüger, C.; Romão, M. J. *Z. Naturforsch., B: Anorg. Chem., Org. Chem.* **1984**, *39B*, 1076. Pörschke, K. R.; Nynott, R. *Z. Naturforsch., B: Anorg. Chem., Org. Chem.* **1984**, *39B*, 1565.
(20) Sacconi, L.; Ghilardi, C. A.; Mealli, C.; Zanobini, F. *Inorg. Chem.* **1975**, *14*, 1380.
(21) Cecconi, F.; Midollini, S.; Orlandini, A. *J. Chem. Soc., Dalton Trans.* **1983**, 2263.

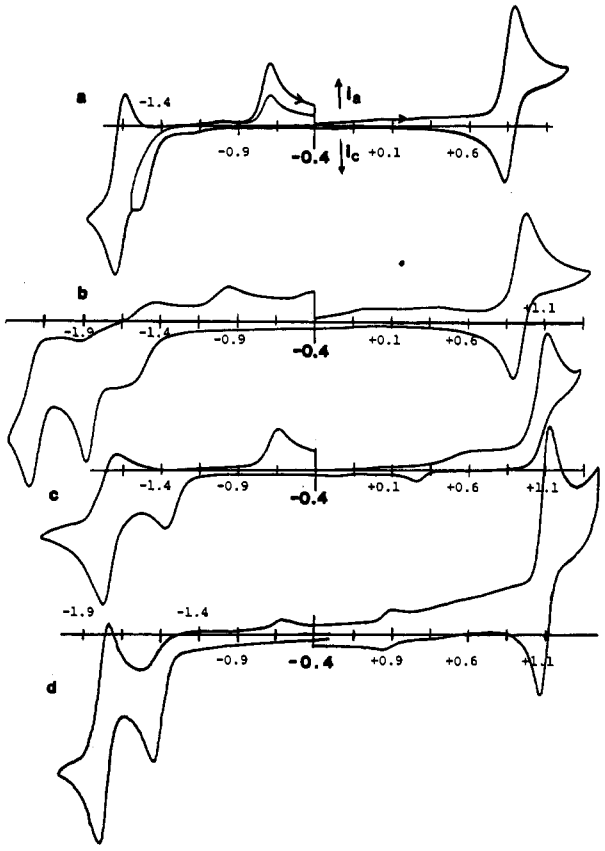

Figure 3. Cyclic voltammograms of 1.0×10^{-3} M solutions of (a) $[Fe(PP_3)(CH_3CN)_2](BF_4)_2$, (b) $[Fe(PP_2)(CH_3CN)_3](BF_4)_2$, (c) $[Fe(dppe)_2(CH_3CN)_2](BF_4)_2$, and (d) $[Fe(dppe)_2(CH_3CN)_2](BF_4)_2$ at −34 °C. The supporting electrolyte solution is 0.3 N NEt_4BF_4 in acetonitrile, and the working electrode is glassy carbon. Scan rates are all 50 mV/s. Each division of the x axis represents 250 mV.

following the oxidation of Fe(II) to Fe(III) is not clear at present, but the wave at +0.85 V is assigned to a one-electron oxidation. This assignment is based on the observation that the peak current for the wave at +0.85 V is 1.05 times that of the Fe(I/0) couple discussed below.

An irreversible cathodic wave is observed at −1.52 V. It has an associated anodic wave at −0.73 V as confirmed by reversing the scan direction before and after the peak is traversed at −1.52 V. Both of these waves are under diffusion control and are assigned to Fe(II/I) couples as shown in Scheme I. The peak current for the cathodic wave at −1.52 V shifts to more cathodic potentials as the cyclic voltammetry measurements are repeated. However, cleaning the electrode surface before each cyclic voltammogram gives reproducible results. A second reversible reduction wave is observed at −1.73 V and is assigned to the Fe(I/0) couple. The 60-mV peak-to-peak separation observed for this wave is consistent with a reversible one-electron-redox process. Exhaustive electrolysis carried out in THF at −1.9 V vs. ferrocene at a mercury pool results in the passage of 1.95 electrons per iron atom. Bulk electrolysis carried out at a carbon rod at the same potential in acetonitrile typically results in a rapid decay of the current after ~1.1 electrons per iron atom have passed. A red-purple precipitate can be observed on inspecting the carbon electrode. The remaining solution is brown. When the solvent is removed from the solution and the product redissolved in THF, an EPR resonance is observed at $g = 2.06$ with unresolved hyperfine splitting as shown in Figure 1c. The observation of an EPR spectrum and the passage of one electron confirm an Fe(I) product. These results are consistent with the electrolysis of $[Fe(PP_3)(CH_3CN)_2](BF_4)_2$ occurring in a stepwise fashion to form first an Fe(I) complex followed by reduction of Fe(I) to Fe(0). The insolubility of the Fe(0) complex in acetonitrile results in precipitation at the carbon electrode and its passivation. The predominant species left in solution is an Fe(I) complex. Reoxidation of a Fe(I) acetonitrile solution generated by bulk electrolysis regenerates $[Fe(PP_3)(CH_3CN)_2](BF_4)_2$ and demonstrates the chemical reversibility of the Fe(II/I) redox couple.

In tetrahydrofuran or acetone solutions, the redox potential of the wave assigned to the reversible Fe(I/0) couple does not depend on the concentration of acetonitrile. This observation coupled with the reversibility of this wave confirms that acetonitrile is neither lost nor gained during this redox process. Since the Fe(0) complex $[Fe(PP_3)(CH_3CN)]$ has been isolated and characterized as a five-coordinate species, the Fe(I) complex can be unambiguously formulated as five-coordinate $[Fe(PP_3)(CH_3CN)](BF_4)$. The potential of the Fe(I/0) wave would be expected to shift as a function of acetonitrile concentration if the Fe(I) complex was involved in an equilibrium between five- and six-coordinate species. The anodic wave at −0.67 V, however, does shift to more negative potentials by about 55 mV upon adding acetonitrile (to make the solution 0.3 M in acetonitrile). This shift is in the direction expected from the Nernst equation[10] since the acetonitrile should rapidly remove the five-coordinate Fe(II) species formed on oxidation as shown in Scheme I. In tetrahydrofuran solutions of $[Fe(PP_3)(CH_3CN)]$, the cathodic wave at −1.52 V is absent. This observation is consistent with the assignment of this wave to the reduction of $[Fe(PP_3)(CH_3CN)_2](BF_4)_2$ since this complex cannot form in the absence of acetonitrile. Addition of acetonitrile to the solution regenerates this wave. In acetone solutions of $[Fe(PP_3)(CH_3CN)_2](BF_4)_2$ this wave does not shift when acetonitrile is added. This observation is consistent with a fast, irreversible loss of acetonitrile from the transient six-coordinate Fe(I) species $[Fe(PP_3)(CH_3CN)_2](BF_4)$ as shown in Scheme I. Since the reaction following the diffusion-controlled electron transfer is irreversible, no dependence on acetonitrile concentration is expected.[10]

Although $[Fe(PP_3)(CH_3CN)]$ is only sparingly soluble in acetonitrile, the cyclic voltammogram of this complex is identical with that of $[Fe(PP_3)(CH_3CN)_2](BF_4)_2$ with the exception that the anodic wave for the Fe(I/II) couple is larger and the corresponding cathodic wave is smaller, as expected. In pure THF a slow decomposition of $[Fe(PP_3)(CH_3CN)]$ occurs with the formation of a new redox active species. The disappearance of $[Fe(PP_3)(CH_3CN)]$ can be conveniently followed by cyclic voltammetry and has a half-life of approximately 20 min. Addition of large amounts of acetonitrile can effectively suppress this process and indicates that dissociation of acetonitrile from $[Fe(PP_3)(CH_3CN)]$ is an important step in this reaction.[22] A similar, but slower reaction is observed for the isoelectronic complex $[Co(PP_3)(CH_3CN)](BF_4)_2$, vida infra.

The cyclic voltammogram for $[Fe(PP_2)(CH_3CN)_3](BF_4)_2$ is shown in Figure 3b. A quasi-reversible, diffusion-controlled, one-electron oxidation is observed at +0.95 V with a peak-to-peak separation of ~90 mV. This separation is similar to that observed for $[Fe(PP_3)(CH_3CN)_2](BF_4)_2$ and $[Fe(dppe)_2(CH_3CN)_2](BF_4)_2$ (Table I). This indicates that the difference in oxidation potentials of the facial and meridional isomers is small. The one-electron nature of the oxidation wave is based on the fact that i_p for the oxidation wave is almost identical with that of $[Fe(PP_3)(CH_3CN)_2](BF_4)_2$, as can be seen from Figure 3. All of the reduction waves of $[Fe(PP_2)(CH_3CN)_3](BF_4)_2$ are irreversible, and no assignments to specific redox processes are made. Apparently a fourth phosphine ligand is needed in the coordination sphere before the Fe(I/0) couple becomes reversible.

Scheme I is also appropriate for $[Fe(dppe)_2(CH_3CN)_2](BF_4)_2$ with only minor modifications. As can be seen from Figure 3c the oxidation of the tetrafluoroborate salt $[Fe(dppe)_2(CH_3CN)_2](BF_4)_2$ is irreversible in a solution of NEt_4BF_4 in

(22) It is well-known that four-coordinate phosphine complexes of Fe(0) are capable of activating C–H bonds as described in the following references. However, it is beyond the scope of this work to determine if such a process is operative here. Antberg, M.; Dahlenburg, L. *Angew. Chem., Int. Ed. Engl.* **1986**, *25*, 260. Tolman, C. A.; Ittel, S. D.; English, A. D.; Jesson, J. P. *J. Am. Chem. Soc.* **1978**, *100*, 4080. Karsch, H. H. *Chem. Ber.* **1984**, *117*, 3123. Rathke, J. W.; Muetterties, E. L. *J. Am. Chem. Soc.* **1985**, *285*, 99.

Table I. Comparison of Cyclic Voltammetry Data for $[ML(CH_3CN)_n](BF_4)_2$ Complexes

complex	$E_{1/2}$ values for indicated changes in oxidn states,[a] V			
	3/2	2/1	1/0	0/−1
$Fe(PP_3)(CH_3CN)_2](BF_4)_2$	+0.85 (80)[b]	−1.52 c, −0.73 a[c] (irr)	−1.73 (60)	
$[Fe(PP_2)(CH_3CN)_3](BF_4)_2$	+0.90 (90)	−1.59 c, −1.70 c, −0.99 a[d] (irr)	−1.94 c, −2.29 c[d] (irr)	
$[Fe(dppe)_2(CH_3CN)_2](BF_4)_2$	+1.05 (90)[e]	−1.51 c, −0.64 a (irr)	−1.79 (140)	
$[Co(PP_3)(CH_3CN)](BF_4)_2$	+0.67 c, −0.16 a (irr)	−0.54 (70)		
$[Co(dppe)_2(CH_3CN)](BF_4)_2$	+1.2 c, −0.13 a	−0.71 (60)	−1.56 (70)	−2.03 (60)
$[Ni(PP_3)(CH_3CN)](BF_4)_2$		−1.03 (100)	−1.28 c (irr)	
$[Ni(PP_2)(CH_3CN)](BF_4)_2$		−0.88 (70)	−1.26 c (irr)	
$[Ni(dppe)_2](BF_4)_2$		−0.71 (60)	−0.89 (60)	

[a] All potentials are reported vs. ferrocene used as an internal standard. See Experimental Section for conversion of these values to values vs. SCE. [b] Values in parentheses indicates peak-to-peak separation (in mV). [c] The letters a and c for irreversible redox waves (irr) indicate whether the peak is anodic or cathodic, respectively. The potentials listed for irreversible couples represent the potential of the peak current and not $E_{1/2}$. [d] The changes in oxidation states associated with these redox waves are not known. [e] See text for discussion of factors influencing reversibility.

acetonitrile. This is surprising since the oxidation of $[Fe(dppe)_2(CH_3CN)_2](ClO_4)_2$ in a solution of NEt_4ClO_4 in acetonitrile is reversible.[3] However, if a cyclic voltammogram is recorded on a solution of $[Fe(dppe)_2(CH_3CN)_2](BF_4)_2$ in a 0.3 N solution of NEt_4ClO_4 in acetonitrile, this oxidation wave becomes much more reversible. In addition, a diffusion-controlled, quasi-reversible wave is observed for even a NEt_4BF_4 solution at −34 °C as shown in Figure 3d. These results are consistent with the Fe(III) complex formed on oxidation reacting with the tetrafluoroborate anion.

The appearance of the two cathodic waves for $[Fe(dppe)_2(CH_3CN)_2](BF_4)_2$ in a solution of NEt_4BF_4 in acetonitrile is the same as reported previously for $[Fe(dppe)_2(CH_3CN)_2](ClO_4)_2$ with NEt_4ClO_4 as the supporting electrolyte.[3] The first reduction wave at −1.51 V is irreversible but diffusion-controlled with an associated diffusion-controlled anodic wave at −0.64 V. These waves are assigned to the electrochemically irreversible but chemically reversible reduction of Fe(II) to Fe(I) and the reoxidation of Fe(I) to Fe(II), respectively. Controlled-potential electrolysis at −1.65 V using a mercury pool or carbon rod as the electrode results in the passage of 1.0 electron per Fe atom and the formation of brown solutions. Cyclic voltammograms of these acetonitrile solutions are the same as observed for Figure 3c except that the cathodic wave at −1.51 V is absent and the anodic wave at −0.64 V is a fully developed one-electron wave. These results confirm the formation of a stable Fe(I) species. Reoxidation of the Fe(I) solutions generated by bulk electrolysis results in the passage of 1.0 electron per Fe atom and the re-formation of $[Fe(dppe)_2(CH_3CN)_2](BF_4)_2$. This demonstrates the chemical reversibility of the Fe(II/I) redox couple.

An EPR spectrum of the Fe(I) product formed in the bulk electrolysis experiments was obtained by removing the acetonitrile solvent in vacuo and dissolving the residue in THF. The EPR spectrum is shown in Figure 1d and consists of a seven-line pattern with appropriate intensities for the equal coupling of the electron to the four phosphorus nuclei and the nitrogen nucleus of the acetonitrile ligand. The observation of coupling to only one nitrogen nucleus is consistent only with a five-coordinate structure since the two acetonitrile ligands would couple equivalently to the electron for either a cis or trans octahedral complex. Thus the EPR spectrum supports the electrochemical results and is consistent with the formation of $[Fe(dppe)_2(CH_3CN)](BF_4)$. The perchlorate salt has been prepared by others and characterized by elemental analysis and magnetic susceptibility measurements as a five-coordinate complex.[3]

The cathodic portion of the second reduction wave has the shape of a reversible reduction, while the anodic portion is broadened and the peak height somewhat less than expected for a truly reversible process. The lack of reversibility of the Fe(I/0) couple at room temperature is due to loss of acetonitrile from $[Fe(dppe)_2(CH_3CN)]$. This interpretation is based on the observation that in THF solutions the Fe(I/0) couple is totally irreversible with no anodic wave being observed. The anodic wave is restored upon addition of large amounts of acetonitrile. The change in the nature of the wave for the Fe(I/0) couple from quasi-reversible in acetonitrile to irreversible in THF is consistent with the loss of acetonitrile. The observation of a fully reversible one-electron wave for the Fe(I/0) couple at low temperature (Figure 3d) indicates a slowing of this process at low temperature. These observations are similar to those for $[Fe(PP_3)(CH_3CN)]$ described above in which acetonitrile loss occurs in THF solutions.

Electrochemical Studies of Co Complexes. The cyclic voltammogram of $[Co(PP_3)(CH_3CN)](BF_4)_2$ in acetonitrile consists of a reversible one-electron reduction at −0.54 V. The oxidation to Co(III) is irreversible with a diffusion-controlled anodic peak at +0.67 V and a kinetically controlled cathodic peak at −0.16 V. Bulk electrolysis of an acetonitrile solution using a carbon electrode as the cathode (−1.1 V vs. ferrocene) results in the passage of 1.0 electron per molecule. A ^{31}P NMR spectrum of the resulting red solution showed a doublet at 58.4 ppm ($^2J_{PP}$ = 35 Hz) and a quartet at 157.2 ppm identical with that of $[Co(PP_3)(CH_3CN)](BF_4)$. Similarly, bulk electrolysis of $[Co(PP_3)(CH_3CN)](BF_4)_2$ at a +0.85 V using reticulated vitreous carbon as the anode results in the passage of 1.1 electrons per molecule. Electrolysis of this solution at −0.3 V results in the passage of 1.0 electron per molecule and regeneration of $[Co(PP_3)(CH_3CN)](BF_4)_2$. The latter result confirms the chemical reversibility of the Co(II/III) couple.

Addition of acetonitrile to dichloromethane solutions of $[Co(PP_3)(CH_3CN)](BF_4)_2$ does not produce any detectable change in the potential of the Co(II/I) couple. These cyclic voltammetry results indicate that there is no rapid loss of acetonitrile on reduction to cobalt(I), as expected. The anodic wave for the oxidation of $[Co(PP_3)(CH_3CN)](BF_4)_2$ shifts in a negative direction as the acetonitrile concentration is increased. This is consistent with the removal of $[Co(PP_3)(CH_3CN)](BF_4)_3$ formed on oxidation by coordination of acetonitrile. This behavior parallels that observed for the Fe(I/II) couple of $[Fe(PP_3)(CH_3CN)](BF_4)$ discussed above.

The cobalt(I) complex $[Co(PP_3)(CH_3CN)](BF_4)$ is also similar to the isoelectronic $[Fe(PP_3)(CH_3CN)]$ complex. The cobalt complex undergoes a slow reaction in dichloromethane to produce a new redox active species with a diffusion-controlled, reversible, one-electron wave at −1.02 V and an irreversible oxidation wave at +0.16 V. The half-life for this reaction is approximately 2.5 h. As in the case of $[Fe(PP_3)(CH_3CN)]$ in THF this reaction is suppressed, but not reversed, by the addition of acetonitrile. These results are consistent with a slow dissociation of acetonitrile to produce a four-coordinate intermediate $[Co(PP_3)](BF_4)$.[23] In the presence of acetonitrile this species can recombine with acetonitrile to regenerate $[Co(PP_3)(CH_3CN)](BF_4)$. In the absence of acetonitrile $[Co(PP_3)](BF_4)$ undergoes an irreversible conversion to a second redox-active species. Thus, the electrochemical and chemical behavior observed for the isoelectronic d^6, d^7, and d^8 complexes of Fe and Co with PP_3 appear to be similar.

The electrochemistry of $[Co(dppe)_2](ClO_4)_2$ in acetonitrile has been reported previously[4] and is the same as that observed for $[Co(dppe)_2(CH_3CN)](BF_4)_2$ as would be expected since both

(23) An analogous complex $[Co(NP_3)](BF_4)$ (where NP_3 is $N(CH_2CH_2PPh_2)_3$) has been structurally characterized. Sacconi, L.; Orlandini, A.; Midollini, S. *Inorg. Chem.* **1974**, *13*, 2850.

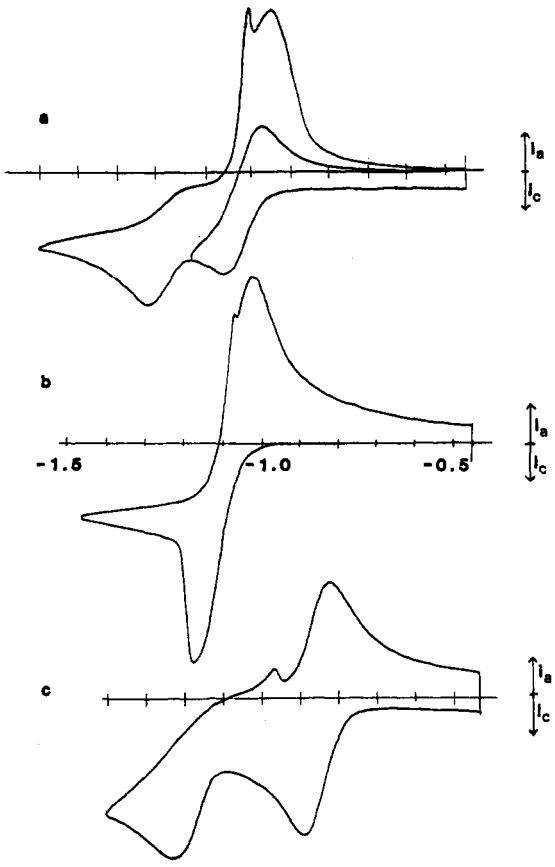

Figure 4. Cyclic voltammograms of (a) a 1.00×10^{-3} M solution of $[Ni(PP_3)(CH_3CN)](BF_4)_2$. (b) a 1.00×10^{-2} M solution of $[Ni(PP_3)(CH_3CN)](BF_4)_2$, and (c) an approximately 1×10^{-3} M solution of $[Ni(PP_2)(CH_3CN)](BF_4)_2$. The supporting electrolyte solution is 0.3 N NEt_4BF_4 in acetonitrile, and the working electrode is glassy carbon. Scan rates are 50 mV/s in each case. Each division of the x axis represents 100 mV.

complexes should exist as the five-coordinate cation $[Co(dppe)_2(CH_3CN)]^+$ in acetonitrile. The electrochemical parameters obtained for $[Co(dppe)_2(CH_3CN)](BF_4)_2$ are reported in Table I for comparison with those obtained for $[Co(PP_3)(CH_3CN)](BF_4)_2$.

Cyclic voltammetry measurements were carried out on an acetone solution of $[Co(dppe)_2(CH_3CN)](BF_4)_2$ at various concentrations of acetonitrile. A plot of $E_{1/2}$ for the cobalt(II/I) couple vs. the log of the concentration of acetonitrile was linear over the range of 2×10^{-3} to 7×10^{-2} M. The slope of 0.050 is consistent with a rapid and reversible loss of one acetonitrile on reduction to cobalt(I).[10] These results are similar to our observations of the electrochemistry of $[Fe(dppe)_2(CH_3CN)](BF_4)$ (vide supra) in which reduction of $[Fe(dppe)_2(CH_3CN)](BF_4)$ in THF was accompanied by loss of acetonitrile.

Electrochemical Studies of Ni Complexes. Traces a and b of Figure 4 are the cyclic voltammograms of 1.0×10^{-3} and 1.0×10^{-2} M solutions of $[Ni(PP_3)(CH_3CN)](BF_4)_2$, respectively. For a 1.0×10^{-3} M solution a diffusion-controlled, quasi-reversible, one-electron reduction is observed at −1.03 V vs. ferrocene, and an irreversible reduction is observed at −1.28 V. At higher concentrations, such as shown in trace b of Figure 4, the second reduction wave becomes associated with electrode passivation and an oxidative spike on potential reversal. That passage of current is blocked at the electrode is indicated by two observations. First, after the Ni(I/0) couple has been traversed the current passed is much smaller than would be expected for a truly diffusive process. Secondly, if $[Fe(PP_3)(CH_3CN)_2](BF_4)_2$ is added to a 5×10^{-3} M solution of $[Ni(PP_3)(CH_3CN)](BF_4)_2$, waves for the Fe(II/I) and Fe(I/0) couples are not observed. This experiment also supports the one-electron nature of the redox process occurring at −1.03 V. If the diffusion coefficients for the Ni and Fe complexes are assumed to be the same, the ratio of i_p for the Fe(II/III) couple to i_p for the wave at −1.03 V is expected to be 0.35 for a two-electron wave. However, the observed ratio is 0.8 and is more consistent with the wave at −1.03 V being a one-electron reduction.

Bulk electrolysis of $[Ni(PP_3)(CH_3CN)](BF_4)_2$ carried out at a mercury pool in acetonitrile at −1.4 V results in the passage of 2.2 electrons per nickel atom and the formation of a yellow solid. The solid was collected by decanting the supporting electrolyte solution and dissolving the solid in THF. A ^{31}P NMR spectrum of the THF solution was identical with that of $[Ni(PP_3)]_2$ prepared from $Ni(COD)_2$ and PP_3. No other products were observed.

Electrochemical measurements on the Ni(I) complex $[Ni(PP_3)](BF_4)$ were not possible since the compound reacts rapidly with chlorinated solvents, is insoluble in THF and related solvents, and disproportionates in acetonitrile to form soluble $[Ni(PP_3)(CH_3CN)](BF_4)_2$ and insoluble $[Ni(PP_3)]_2$. Both of these products were identified by ^{31}P NMR spectroscopy.

The cyclic voltammogram of $[Ni(PP_2)(CH_3CN)](BF_4)_2$ shown in trace c of Figure 4 consists of a reversible one-electron reduction at −0.88 V and an irreversible one-electron reduction at −1.26 V. The one-electron nature of the first wave is indicated by a 70-mV peak-to-peak separation. Under the same conditions ferrocene has a 65-mV peak-to-peak separation. Bulk electrolysis at −1.0 V in acetonitrile at a mercury pool results in the passage of 1.0 electron per nickel atom. The nature of the Ni(I) products formed is not known and no EPR spectrum is observed. The small wave observed at −0.99 V is associated with the Ni(I/0) redox couple since this wave is not observed unless the wave at −1.26 V is traversed. This wave does not have the shape of a typical diffusion wave, and its origin is probably due to precipitation of a Ni(0) complex in a phenomenon similar to that observed for $[Ni(PP_3)(CH_3CN)](BF_4)_2$.

Discussion and Summary

In the research described above a general approach has been demonstrated for the synthesis of (polyphosphine)metal complexes containing weakly coordinating acetonitrile ligands. This synthetic method has been utilized to systematically prepare Fe, Co, and Ni complexes containng tetradentate, tridentate, and bidentate phosphine ligands. Only the reaction of $[Co(CH_3CN)_6](BF_4)_2$ with PP_2 failed to yield an analytically pure complex.

Table I lists the cyclic voltammetry data for compounds prepared in this work. It can be seen from this table that the nature of the polyphosphine ligand has a significant effect on the electrochemistry observed for a particular metal. All of the iron complexes exhibit an oxidation wave and two or more reduction waves. Only for $[Fe(PP_3)(CH_3CN)_2](BF_4)_2$ are both the Fe(II/III) and Fe(I/0) couples reversible or quasi-reversible. For $[Fe(PP_2)(CH_3CN)_3](BF_4)_2$ the Fe(II/III) couple is quasi-reversible, but all reductions are irreversible. For $[Fe(dppe)_2(CH_3CN)_2](BF_4)_2$ the Fe(II/III) couple is irreversible, and the Fe(I/0) couple is followed by a chemical reaction that involves loss of acetonitrile. The electrochemical reversibility of the Fe(I/0) couple of $[Fe(PP_3)(CH_3CN)_2](BF_4)_2$ indicates that $[Fe(PP_3)(CH_3CN)]$ does not lose acetonitrile as readily subsequent to formation as does $[Fe(dppe)_2(CH_3CN)]$. This is a general trend that is also observed for Co(I) and Ni(II) complexes of PP_3 and dppe. In polar, noncoordinating solvents, $Ni(dppe)_2^{2+}$ and $Co(dppe)_2^+$ are four-coordinate complexes.[18,24] However, the isoelectronic $[Ni(PP_3)(CH_3CN)](BF_4)_2$, $[Co(PP_3)(CH_3CN)](BF_4)$, and $[Fe(PP_3)(CH_3CN)]$ complexes are five-coordinate. This stronger affinity of the d^8 complexes of the PP_3 ligand for a fifth ligand is the origin of the greater electrochemical reversibility of the Fe(I/0) couple of $[Fe(PP_3)(CH_3CN)](BF_4)$ compared to $[Fe(dppe)_2(CH_3CN)]BF_4$.

Although $[Co(dppe)_2(CH_3CN)](BF_4)_2$ exhibits three reversible reduction waves, $[Co(PP_3)(CH_3CN)](BF_4)_2$ has only one reduction wave observable in acetonitrile. The failure to observe further reduction of $[Co(PP_3)(CH_3CN)](BF_4)_2$ is attributed to structural constraints imposed by the PP_3 ligand. The d^9 complex

(24) Nobile, C. F.; Rossi, M.; Sacco, A. *Inorg. Chim. Acta* **1971**, *5*, 698.

$[Co(dppe)_2]$ would be expected to have a D_{2d} structure lying between square planar and tetrahedral. In contrast, PP_3 would be expected to impose a pyramidal structure on $[Co(PP_3)]$ as is observed for $[Ni(PP_3)](ClO_4)$.[21] Since the pyramidal geometry is energetically less favored than a D_{2d} geometry, the corresponding reduction would be expected to be more difficult.

For nickel(II), the PP_3 ligand stabilizes a five-coordinate trigonal-bipyramidal structure, while dppe and PP_2 form four-coordinate square-planar complexes. For all three nickel complexes three oxidation states are available in the potential range of −0.7 to −1.3 V vs. ferrocene, and all exhibit a reversible or quasi-reversible one-electron wave for the Ni(II/I) couple. The Ni(I/0) couple is reversible for $[Ni(dppe)_2](BF_4)_2$ and irreversible for $[Ni(PP_3)(CH_3CN)](BF_4)_2$ and $[Ni(PP_2)(CH_3CN)](BF_4)_2$. For $[Ni(PP_3)(CH_3CN)](BF_4)_2$ the irreversibility of the Ni(I/0) couple is due to a ring opening process in which a metal–phosphorus bond is broken and a Ni(0) dimer, $[Ni(PP_3)]_2$, is formed. The rupture of the nickel–phosphorus bond is attributed to ring strain in the transient pyramidal $[Ni(PP_3)]$ complex. In contrast, $[Ni(dppe)_2](BF_4)_2$ is free to distort to a tetrahedral structure on reduction, and the Ni(I/0) couple is reversible. For $[Ni(PP_2)(CH_3CN)](BF_4)_2$ the irreversibility of the Ni(I/0) couple probably arises from loss of acetonitrile on reduction to Ni(0).

Acknowledgment. This research was supported by the U.S. Department of Energy, Office of Basic Energy Sciences, Division of Chemical Sciences. Helpful discussions with Dr. John Turner are also gratefully acknowledged.

Contribution from the Department of Chemistry, Furman University, Greenville, South Carolina 29613

Synthesis, Characterization, and Photobehavior of Macrocyclic Difluoro Complexes of Chromium(III)

Noel A. P. Kane-Maguire,* Kevin C. Wallace, and David G. Speece

Received June 11, 1986

The Cr(III) complexes *cis*-$[Cr(cyclam)F_2]ClO_4$ and *trans*-$[Cr(tet\ a)F_2]ClO_4$, where cyclam and tet a are the macrocyclic tetraamines 1,4,8,11-tetraazacyclotetradecane and *C-meso*-5,7,7,12,14,14-hexamethyl-1,4,8,11-tetraazacyclotetradecane, respectively, have been synthesized by refluxing the macrocycle in methoxyethanol with *trans*-$[Cr(py)_4F_2]ClO_4$. The cis complex is quite photoactive in room-temperature aqueous solution (ϕ_{F^-} = 0.24 (350-nm excitation), 0.28 (514.5-nm excitation); ϕ_{cyclam} = 0). These results contrast sharply with the photobehavior observed for the analogous nonmacrocyclic complex *cis*-$Cr(NH_3)_4F_2^+$ (ϕ_{NH_3} = 0.45; $\phi_{F^-} < 0.06$) but are in accord with the preferential F^- loss previously noted for $Cr(tren)F_2^+$ (tren = β,β′,β″-triaminotriethylamine). Normal $^2E_g \rightarrow {}^4A_{2g}$ (O_h) phosphorescence is observed from *cis*-$Cr(cyclam)F_2^+$, but only weakly in room-temperature solution. In contrast, the corresponding tet a species *trans*-$[Cr(tet\ a)F_2]ClO_4$ is photoinert on ligand field excitation and exhibits relatively intense, long-lived $^2T_{1g} \rightarrow {}^4A_{2g}$ (O_h) phosphorescence in room-temperature solution. Furthermore, under the same experimental conditions this trans complex displays an 8-fold increase in both its steady-state emission intensity and lifetime on N–H deuteriation ($\tau_{undeutd}$ = 30 μs; τ_{deutd} = 234 μs; 20 °C, acidified aqueous solution). The presence of a *solvent*-deuterium isotope effect ($\tau_{deutd(H_2O)}$ = 234 μs; $\tau_{deutd(D_2O)}$ = 430 μs; 20 °C) indicates contributions to $^2T_{1g} \rightsquigarrow {}^4A_{2g}$ (O_h) relaxation in room-temperature solution from vibrational coupling with the solvent. The contrast in photobehavior between *trans*-$Cr(tet\ a)F_2^+$ (photoinert, long-lived emission) and its nonmacrocyclic counterpart *trans*-$Cr(en)_2F_2^+$ (photolabile, short-lived emission) is discussed with reference to possible pathways for doublet excited-state deactivation.

Introduction

We have recently noted[1] the striking difference in photobehavior between the cis and trans isomers of the Cr(III) complex $Cr(cyclam)(NH_3)_2^{3+}$, where cyclam is the macrocyclic tetradentate amine ligand 1,4,8,11-tetraazacyclotetradecane. The trans isomer is characterized by a near absence of discernible photochemistry and an exceptionally intense, long-lived $^2A_{1g}$, $^2B_{1g} \rightarrow {}^1B_{1g}$ (D_{4h}) phosphorescence that exhibits a strong N–H deuterium isotope effect in room-temperature solution. In contrast, the cis species under comparable conditions is photochemically active (ϕ_{NH_3} = 0.2) and displays a much shorter lived phosphorescence signal and a weak deuterium isotope effect. These observations and related data[2] for *trans*-$Cr(cyclam)(CN)_2^+$ have provided support for a viewpoint that argues for a *direct* photochemical role for the ^2E_g (O_h) excited state of corresponding nonmacrocyclic complexes such as $Cr(NH_3)_6^{3+}$ and *trans*-$Cr(en)_2(CN)_2^+$.

In each of these cases it was suggested that $^2E_g \rightsquigarrow {}^4T_{2g}$ (O_h) back-intersystem crossing (back-ISC) was relatively unimportant as a ^2E_g deactivation pathway at room temperature, due to the substantial activation barrier anticipated.[1-3] However, many Cr(III) systems are expected to have significantly smaller barriers to ^2E_g back-ISC, and the photochemical role of the ^2E_g state could prove even more difficult to assess. Difluoro complexes of the general type *cis*/*trans*-$Cr(N_4)F_2^+$ belong to this latter category of species[4,5] and have been the subject of considerable prior study.[6-14] As part of our continuing study of the photobehavior of complexes with macrocyclic ligands, we have therefore investigated several analogous difluoro Cr(III) complexes containing macrocyclic tetradentate amine ligands. This report describes

(1) Kane-Maguire, N. A. P.; Wallace, K. C.; Miller, D. B. *Inorg. Chem.* **1985**, *24*, 597.
(2) Kane-Maguire, N. A. P.; Crippen, W. S.; Miller, P. K. *Inorg. Chem.* **1983**, *22*, 696, 2972.
(3) Ramasami, T.; Endicott, J. F.; Brubaker, G. R. *J. Phys. Chem.* **1983**, *87*, 5057. Endicott, J. F. *J. Chem. Educ.* **1983**, *60*, 824.
(4) Kirk, A. D.; Porter, G. B. *J. Phys. Chem.* **1980**, *84*, 887.
(5) Linck, N. J.; Berens, S. J.; Magde, D.; Linck, R. G. *J. Phys. Chem.* **1983**, *87*, 1733.
(6) Pyke, S. C.; Linck, R. G. *J. Am. Chem. Soc.* **1971**, *93*, 5281; *Inorg. Chem.* **1980**, *19*, 2468.
(7) Manfrin, M. F.; Sandrini, D.; Juris, A.; Gandolfi, M. T. *Inorg. Chem.* **1978**, *17*, 90.
(8) Kirk, A. D.; Frederick, L. A. *Inorg. Chem.* **1981**, *20*, 60.
(9) Saliby, M. J.; Sheridan, P. S.; Madan, S. K. *Inorg. Chem.* **1980**, *19*, 1291.
(10) Vanquickenborne, L. G.; Ceulemans, A. *J. Am. Chem. Soc.* **1977**, *99*, 2208; **1978**, *100*, 475; *Inorg. Chem.* **1979**, *18*, 3475.
(11) Flint, C. D.; Matthews, A. P. *J. Chem. Soc., Faraday Trans. 2* **1974**, *70*, 1307.
(12) DeCurtins, S.; Gudel, H. U.; Neuenschwander, K. *Inorg. Chem.* **1977**, *16*, 796.
(13) Forster, L. S.; Rund, J. V.; Fucaloro, A. F. *J. Phys. Chem.* **1984**, *88*, 5012.
(14) Fucaloro, A. F.; Forster, L. S.; Glover, S. G.; Kirk, A. D. *Inorg. Chem.* **1985**, *24*, 4242.

0020-1669/86/1325-4650$01.50/0